Simplified Orientation Determination in Ski Jumping using Inertial Sensor Data

B.H. Groh[1], N. Weeger[1], F. Warschun[2], B.M. Eskofier[1]

[1] Digital Sports Group, Pattern Recognition Lab
University of Erlangen-Nürnberg (FAU)
Martensstr. 3
91058 Erlangen
GERMANY

[2] University of Leipzig
Ritterstr. 26
04109 Leipzig
GERMANY

Inertial Sensors and Systems 2014
Karlsruhe, Germany

Abstract

The determination of the orientation of the skis during ski jumping provides fundamental information for athletes, coaches and spectators. Athletes and coaches can improve the training and the jump performance. Spectators can obtain interesting facts and a more attractive way of jump visualization by an orientation and jump angle determination. Existing camera-based systems to determine jump angles require a complex setup and calibration procedure. In contrast, inertial sensor-based methods can provide similar information with a low-cost and easy maintainable sensor setup. In this paper, we describe the processing of inertial sensor data (3D accelerometer, 3D gyroscope) in order to obtain the 3D orientation of the skis of an athlete during the whole jump sequence. Our methods include a functional sensor calibration to deal with sensor misalignment and a quaternion-based processing of sensor data. Acceleration data are used to determine the start and end of the jump and specific periods for the functional calibration. Gyroscope data are used to obtain the current orientation of the skis in each step of the movement. The orientation determination is evaluated by comparing the IMU calculated angle of attack (pitch angle of moving system) with a high-speed camera system. Our results show a root mean square error of 2.0° for the right ski and 9.3° for the left ski. It can be assumed that this difference of accuracy is influenced by the simple 2D evaluation method and perspective-related errors. A 3D high-speed video system with an accurate 3D representation of the skis is discussed for further evaluation.

1. Introduction

1.1. Motivation

New inertial sensor based methods of motion analysis in ski jumping provide enhanced performance feedback and demonstrative visualization possibilities. One major aspect of the motion analysis is given by the determination of the 3D orientation of the skis. The pose of the skis during a jump is mainly presented by the angle of attack (often defined as angle between ski and horizontal plane), V-angle (opening angle between both skis) and body-ski-angle (between ski and shank) [1]. These angles directly influence the absolute jump length [2]. Therefore, an accurate angle determination at all times during a jump can provide fundamental information for further investigations in sports science. Furthermore, 3D orientation determination can be used for a visualization of the jumper’s pose during the jump and to establish a more attractive way of presenting the jump to spectators.

1.2. Related work

Schwameder [3] provided a description of ski jumping phases and performance enhancement methods. The main focus was on the influence of the V-technique (jump with V-opening angle) on the jump performance. Chardonnens et al. [4] introduced a system to analyze different parameters of ski jumping. Based on a wearable inertial sensor system, they detected specific temporal features during the jump and calculated the orientation of different body segments. In [5], Chardonnens et al. furthermore presented a more detailed IMU-based determination of the ski and body orientation. Sensors were attached to the skis and the body of athletes and the angular movement was calculated by the obtained angular rate data. A functional calibration was performed before the start of the jump to compensate sensor misalignments. The evaluation of that work was based on the slope at the landing position and on the comparison to typical angles in ski jumping literature. There was no evaluation performed during the actual jump.

Further approaches to determine jump angles without using IMU were proposed by Virmavirta et al. [6] and Schmölzer et al. [7]. Virmavirta et al. [6] monitored the take-off phase of different jumps with two high-speed cameras. Their sports science based investigation was focused on the influence of different jump parameters (e.g. body and ski orientation) on the jump length. Schmölzer et al. [7] obtained the body angles and angle of attack of several jumps measured by eleven video cameras along the flight path. They analyzed the flight styles of different athletes in consideration of the according jump lengths.

The aforementioned projects considered IMU- and camera-based approaches to determine jump-related angles during the jump sequence. However, none of them combined both by e.g. evaluating the IMU-based approach with a high-speed camera system. The method proposed in our work provides an orientation determination of the skis during the whole jump phase. It is evaluated by comparing one angle (the angle of attack) with a 2D high-speed camera system in the take-off phase. The proposed algorithm does not require any additional calibration before the jump but uses specified scenarios of the jump to correct possible misalignments. Thereby, the application in high-class competitions could be simplified.

2. Methods

2.1. Sensor hardware and data collection

The development and evaluation of the proposed algorithm was based on data of a ski jumping training in Oberhof, Germany. Young professional athletes (13 to 14 years) of the sports boarding school 'Sportgymnasium Oberhof' executed several jumps at a K66 ski-jump venue [8]. The data used in this work were obtained by three jumps of one athlete. They were recorded with Shimmer 2 inertial sensors (Shimmer Research, Dublin, Irland) [9] at a sampling rate of 204.8 Hz. The sensors contained a three-axes accelerometer (range: ±6 g) and a three-axes gyroscope (range: ± 500 °/s). The sensor weight was determined to be approximately 28.5 g each. The sensors were attached to both skis behind the binding. Seconds before the jump, the data recording was started and the jump data were stored on the sensor's internal memory. A high-speed video camera (CASIO Exilim EX-ZR200) with a frequency of 240 fps was used as reference system. The resolution was set to the possible maximum of 512x384 pixels. The camera was built up stationarily covering an area of approximately 10 m from the take-off position. The Shimmer 2 inertial sensors and the camera system were synchronized manually for each jump. Therefore, a short-time bending of the skis at the take-off instant and the thereby resulting peak in the acceleration signal were used.

2.2. Initial sensor calibration

The Shimmer 2 sensors were calibrated by the 'Shimmer 9D Calibration Application' on the day of the data acquisition. The application provided the basic parameters that were necessary for the inertial sensor calibration: an offset and a scale factor of the measurement of each axis. The offset of an accelerometer can be assumed to be constant over weeks or even months. In contrast, the gyroscope offset could change within minutes. Therefore, a recalibration of the gyroscope offset was necessary before each jump in order to avoid sensor drift. Considering the practical case, each athlete rests for a few seconds before starting to slide down the ski-jump. That rest state was determined manually by analyzing the stored accelerometer and gyroscope signal. While the athlete did not move the skis, the gyroscope was supposed to detect zero degrees per second as angular velocity on all axes. The actual measured values of all axes were considered as part of the sensor offset and subtracted from the signal for the whole jump sequence. Each jump sequence lasted less than 10 s. The influence of gyroscope drift was ignored for this short duration.

2.3. Functional alignment calibration

Besides the basic sensor calibration, the sensor alignment had to be considered for an accurate signal processing. Therefore, the measurement axes of the sensors were approximately aligned with the ski axes (see Figure 1). The sensor's x-axis was supposed to represent the movement axis of the ski. However, an exact alignment of the sensor axes and the ski axes was not guaranteed as the sensor attachment did not take place under controlled lab conditions. One option to correct for misalignments is to perform a calibration with additional equipment and a specified procedure before each jump. Our simplified approach did neither require any additional equipment nor calibrating procedure. The a-priori knowledge of the jump procedure itself and the structure of the ski-jump was sufficient to account for misalignments between the sensor and ski axes. The functional calibration of the sensor was established by a rotation from the sensor coordinate system (measurement frame) to the ski coordinate system (body frame). The information of three known states was necessary to obtain that rotation. In our approach, the known states were provided by (a) the gravity vector at the initial rest position (two-dimensional information) and (b) the rotation of the descent trajectory before reaching the jump-off platform (third necessary component).

2.3.1. Initial rest state, gravity vector alignment

The slope of the ski-jump φ_{init} (here: $\varphi_{init} = 35°$ [8]) and the acceleration measurement $\boldsymbol{a}_{rest}$ in the rest state provided information about the orientation of the sensor relatively to the ski-jump. In a first step, the sensor's measurement frame was projected to the plane of the

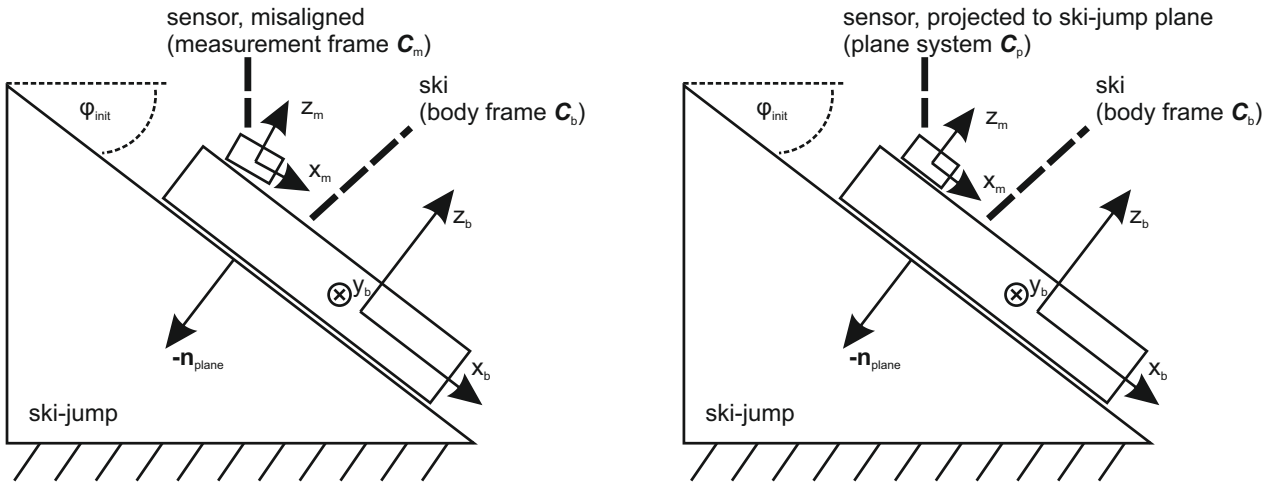

Figure 1. Sideview of ski-jump showing one ski (body frame $\boldsymbol{C}_b$) and the attached sensor (measurement frame $\boldsymbol{C}_m$). Initial state (left): Sensor is misaligned in three dimensions. State after first alignment step (right): Sensor is projected to ski-jump plane $\boldsymbol{C}_p$ but due to a possible rotation in the x-y-plane not yet aligned with body frame.

ramp. That plane was defined by the norm vector $\boldsymbol{n}_{\text{plane}}$ that was given by the slope φ_{init} (Figure 1, left) and the normalized acceleration measurement $\hat{\boldsymbol{a}}_{\text{rest}}$.

Three coordinate systems were used: the body frame of the ski $\boldsymbol{C}_{\text{b}}$, the measurement frame $\boldsymbol{C}_{\text{m}}$ and the plane coordinate system $\boldsymbol{C}_{\text{p}}$ that was set parallel to the ramp. Thereby, the plane coordinate system had the same z-axis as the body frame but different x- and y-axes. The measurement frame $\boldsymbol{C}_{\text{m}}$ was defined by the base vectors

$$\boldsymbol{C}_{\text{m}} = \left[\boldsymbol{x}_{\text{m}} \boldsymbol{y}_{\text{m}} \boldsymbol{z}_{\text{m}}\right] = \left[\begin{pmatrix} 1 \\ 0 \\ 0 \end{pmatrix} \begin{pmatrix} 0 \\ 1 \\ 0 \end{pmatrix} \begin{pmatrix} 0 \\ 0 \\ 1 \end{pmatrix}\right]. \tag{1}$$

The plane coordinate system $\boldsymbol{C}_{\text{p}}$ was defined relatively to $\boldsymbol{C}_{\text{m}}$.

$$\boldsymbol{C}_{\text{p}} = \left[\boldsymbol{x}_{\text{p}} \boldsymbol{y}_{\text{p}} \boldsymbol{z}_{\text{p}}\right] \tag{2}$$

with

$$\begin{aligned} \boldsymbol{z}_{p} &= \boldsymbol{n}_{\text{plane}} \\ \boldsymbol{x}_{\text{p}} &= \boldsymbol{x}_{\text{m}} - \left\langle \boldsymbol{x}_{\text{p}}, \boldsymbol{z}_{\text{p}} \right\rangle \cdot \boldsymbol{z}_{\text{p}} \\ \boldsymbol{y}_{\text{p}} &= \boldsymbol{z}_{\text{p}} \times \boldsymbol{x}_{\text{p}} \end{aligned} \tag{3}$$

$\boldsymbol{z}_{\text{p}}$ was assumed to represent the norm vector n_{plane} as the sensor was supposed to be projected to the ramp. $\boldsymbol{x}_{\text{p}}$ was calculated by a projection of $\boldsymbol{x}_{\text{m}}$ to the plane and $\boldsymbol{y}_{\text{p}}$ was calculated by the cross product of $\boldsymbol{z}_{\text{p}}$ and $\boldsymbol{x}_{\text{p}}$.

The rotation matrix $\boldsymbol{R}_{m}^{p}$ from the measurement frame to the plane frame at the initial rest state was calculated by $\boldsymbol{C}_{\text{m}}$ and $\boldsymbol{C}_{\text{p}}$. All further accelerometer and gyroscope measurements were adjusted using $\boldsymbol{R}_{m}^{p}$.

2.3.2. Descent trajectory, rotation vector alignment

The previous alignment set the sensor to an orientation parallel to the ramp. Hence, the z-axis of the sensor could be assumed to only detect the influence on or around the z-axis of the ski (Figure 1, right). However, the sensor was still misaligned in the x-y-plane and the angle φ_{xy} (Figure 2, left) had to be determined. Therefore, the second fixed scenario of descending the ramp was considered. For physical constraints during the descent sequence, only a rotation of the ski around one axis (here: around the y-axis) is allowed.

Hence, the ideal rotation could be defined to only be measurements on that axis. Due to the misalignment, the rotation was actually measured partially on the x- and on the y-axis and resulted in a measurement vector $\boldsymbol{v}_{\text{meas,gyro}}$. The ideal rotation vector $\boldsymbol{v}_{\text{ideal,gyro}}$ was

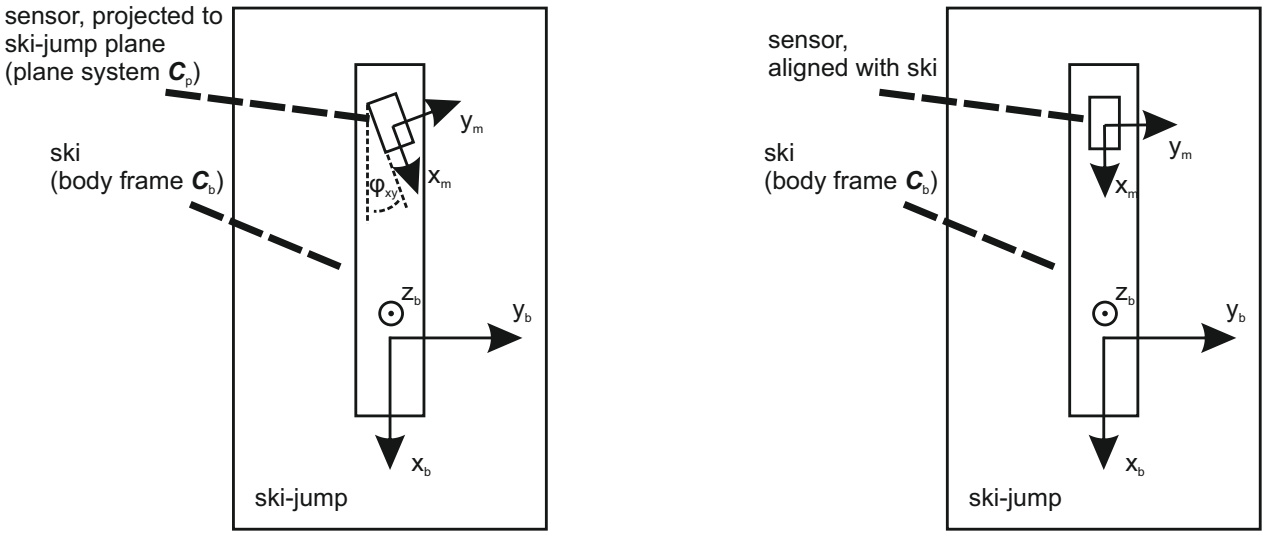

Figure 2. Topview of ski-jump showing one ski (body frame $\boldsymbol{C}_b$) and the attached sensor (measurement frame $\boldsymbol{C}_m$). State after first alignment step (left): Sensor is projected to plane but still misaligned in the x-y-plane. Final state (right): Sensor system is aligned with ski system.

calculated by transforming the whole rotation to the y-axis.

φ_{xy} was determined as the angle between $\boldsymbol{v}_{meas,gyro}$ and $\boldsymbol{v}_{ideal,gyro}$. The resulting rotation $\boldsymbol{R}_p^b$ from the plane coordinate system to the final body frame of the ski movement was calculated and applied to the whole data set.

2.4. Quaternion-based integration of gyroscope data

All quaternions $\boldsymbol{q}$ used in this work were defined by a scalar part q^0 followed by a complex part $q^{\{1,2,3\}}$. At the initial rest state $t = 0$, an initial quaternion $\boldsymbol{q}_0$ without any rotation was set to

$$\boldsymbol{q}_0 = \begin{pmatrix} 1 \\ 0 \\ 0 \\ 0 \end{pmatrix}. \tag{4}$$

At each following time step t, the (already aligned) three-axes gyroscope measurement vector $\boldsymbol{v}_{t,gyro}$ was processed. The rotation during one time step was assumed to be linear. By this assumption, the absolute angular rotation of each step φ_t could be determined by the norm of the integration of the angular rotation vector $\boldsymbol{v}_{t,gyro}$.

$$\varphi_t = \left\| \int \boldsymbol{v}_{t,gyro}\, dt \right\| \tag{5}$$

In addition, the rotation vector $\boldsymbol{\omega}_t$ of the rotation at one time step t was assumed to be the unit vector of the angular rotation $\hat{\boldsymbol{v}}_{t,gyro}$.

$$\boldsymbol{\omega}_t = \begin{pmatrix} \omega_t^x \\ \omega_t^y \\ \omega_t^z \end{pmatrix} = \hat{\boldsymbol{v}}_{t,gyro} \tag{6}$$

Following the basic quaternion definition, the quaternion representing the rotation at *t* was calculated to

$$\boldsymbol{q}_t = \begin{pmatrix} q_t^0 \\ q_t^1 \\ q_t^2 \\ q_t^3 \end{pmatrix} = \begin{pmatrix} \cos(\frac{1}{2}\varphi_t) \\ \omega_t^x \cdot \sin(\frac{\varphi_t}{2}) \\ \omega_t^y \cdot \sin(\frac{\varphi_t}{2}) \\ \omega_t^z \cdot \sin(\frac{\varphi_t}{2}) \end{pmatrix}. \tag{7}$$

By multiplying the current quaternion $\boldsymbol{q}_t$ to all former quaternions, the overall rotation $\boldsymbol{Q}_0^t$ from the initial state *t* = 0 to the current state *t* was determined. An overview of quaternions, quaternion-based rotation sequences and the explanation of quaternion-related mathematics is provided in [10].

2.5. Evaluation: comparison of ski angle of attack

For further processing and evaluating the system, the angle of attack γ (pitch angle of the motion system) was computed as representation for the whole orientation determination. Therefore, the initial orientation of the ski was represented by a vector $\boldsymbol{v}_{init,ski}$. That orientation implied the ski-jump slope at the rest state φ_{init} without any additional rotation of the ski movement. For every time *t* of the jump, the current ski orientation was

Figure 3. One high-speed camera frame used for the angle of attack determination. The angle of attack is defined by the ski orientation and the horizontal plane. Hence, it is calculated by [90° - measured angle in camera frame].

determined by rotating the vector $\boldsymbol{v}_{init,ski}$ by the rotation $\boldsymbol{Q}_0^t$. The resulting vector $\boldsymbol{v}_{t,ski}$ was a three-dimensional representation of the ski.

For the evaluation of the IMU-based angle determination, the available high-speed camera was positioned perpendicularly to the

ski-jump (perspective of Figure 1), facing the x-z-plane of the aligned ski and sensor system. During the take-off period of each evaluated jump, 7 camera frames were chosen manually and the visible pitch angle $\theta_{t,camera}$ of the ski was obtained (see example frame in Figure 3). In order to compare the IMU computation with the camera measurement, the rotated ski vector $\boldsymbol{v}_{t,ski}$ was projected to the x-z-plane and the IMU based angle $\theta_{t,IMU}$ was calculated for the same intervals as the camera frame evaluation by

$$\theta_{t,IMU} = atan\left(\frac{\boldsymbol{v}^z_{t,ski}}{\boldsymbol{v}^x_{t,ski}}\right). \quad (8)$$

3. Results

Three jumps were analyzed by the IMU-based calculation and the camera-based determination of the angle of attack. The difference between both systems was averaged for each jump using a root mean square (RMSE) calculation. The results for the difference $\theta_{t,camera} - \theta_{t,IMU}$ are shown in Table 1.

Table 1: Results of camera-based evaluation

	left ski		**right ski**	
jump	RMSE [°]	std.dev. [°]	RMSE [°]	std.dev. [°]
1	6.7	1.4	1.2	1.3
2	7.2	1.9	2.5	2.3
3	14.1	2.0	2.4	2.5
Ø	**9.3**	**1.8**	**2.0**	**2.0**

4. Discussion and future work

The results showed a considerable difference between the measurements of the left and the right ski. That fact could be explained by the 2D evaluation system inaccuracy. The evaluation system was based on only one camera and deviating perspective-related errors in analyzing the left and the right ski could be expected. However, the similar standard deviation for both skis pointed out a stable performance of the IMU-based algorithm. It could be assumed that better results for the RMSE of the left ski could be obtained with a different evaluation system that does not suffer from perspective-related drawbacks. Furthermore, the result of 2° in RMSE and standard deviation could be explained by the low resolution of the camera. Considering the evaluated camera frame example in Figure 3, an inaccuracy of 2° is understandable. In addition, the chosen camera perspective only allowed an evaluation of one angle that represented the whole orientation. An advanced evaluation of the overall orientation is outstanding. Therefore, a motion capture system with more than one camera is required [11]. The camera frames should be fused to e.g. obtain 3D positions of markers on the skis. An advanced evaluation could also consider the whole jump phase instead of only the take-off period. Therefore, high-resolution cameras will be necessary. Furthermore, a phase detection approach as suggested in [12] could be implemented to automatically detect specific periods of the jump for the functional calibration.

5. Conclusion

In this work, data was acquired by inertial sensors attached behind the bindings of the skis of a ski jumper. The misalignment of that attachment was calculated by a functional calibration during typical scenarios of a jump. The implemented algorithm did not require any additional calibration procedure and thereby simplified the application in high-class competitions. Angular rate data were integrated by a quaternion-based approach to obtain the 3D orientation of both skis at all times. For the evaluation of the algorithm, the angle of attack was calculated for several time steps during the take-off phase and compared to a camera-based angle determination. The evaluation of both skis showed deviating results for both skis, which was explained by the evaluating camera system. With an advanced outdoor motion capture system, more accurate results could be achieved and further investigations based on the accurate angle determination could be established.

References

[1] J. Vodičar et al., “Kinematic structure at the early flight position in ski jumping”, *Journal of human kinetics*, vol. 35, no. 1, pp. 35-45, 2012

[2] B. Schmölzer, W. Müller, “The importance of being light: aerodynamic forces and weigth in ski jumping”, *Journal of biomechanics*, vol. 35, no. 8, pp. 1059-1069, 2002

[3] Schwameder, “Biomechanics research in ski jumping, 1991-2006”, *Sports Biomechanics*, vol. 7, no. 1, pp. 114-136, 2008

[4] J. Chardonnens et al., “Analysis of stable flight in ski jumping based on parameters measured with a wearable system“, in *Proceedings of the 28th International Symposium on Biomechanics in Sports*, pp. 273-276, 2010

[5] J. Chardonnens et al., “A system to measure the kinematics during the entire ski jump sequence using inertial sensors“, *Journal of biomechanics*, vol. 46, no. 1, pp. 56–62, 2013

[6] M. Virmavirta et al., “Take-off analysis of the Olympic ski jumping competition (HS-106m)“, *Journal of biomechanics*, vol. 42, no. 8, pp. 1095-1101, 2009

[7] B. Schmölzer, W. Müller, “Individual flight styles in ski jumping: results obtained during Olympic Games competitions”, *Journal of biomechanics*, vol. 38, no. 5, pp. 1055-1065, 2005

[8] [Online] available: 2014 September 1st
International Ski Federation, “Certificate of jumping hill“
http://www.twz-oberhof.de/data/uploads/sp_amwadeberg_k66.pdf

[9] A. Burns et al., “Shimmer™–a wireless sensor platform for noninvasive biomedical research”, *IEEE Sensors Journal*, vol. 10, no. 9, pp. 1527-1534, 2010

[10] J.B. Kuipers, “Quaternions and rotation sequences”, in *Proceedings of the 1. International Conference on Geometry, Integrability and Quantization*, pp. 2127-143, 1999

[11] T.B. Moeslund et al., “A survey of advances in vision-based human motion capture and analysis“, *Computer vision and image understanding*, vol. 104, no. 2, pp. 90-126, 2006

[12] J. Chardonnens et al., “Automatic measurement of key ski jumping phases and temporal events with a wearable system“, *Journal of sports sciences, vol.* 30, no. 1, pp. 53–61, 2012